NUCLEAR INSTRUMENTS AND METHODS 100 (1972) 179–191; © NORTH-HOLLAND PUBLISHING CO.

ANALYSIS OF POTENTIAL DISTRIBUTION IN A GASEOUS COUNTER OF RECTANGULAR CROSS-SECTION

T. TOMITANI

National Institute of Radiological Sciences, 9–1, 4-Chome, Anagawa, Chiba-shi, 280, Japan

Received 7 June 1971 and in revised form 14 October 1971

The potential in a gaseous counter of rectangular cross-section can be expressed in an analytical form by means of conformal transformation of the Jacobian elliptic function. Equipotential lines and lines of force are calculated numerically for three cases. The potential in a gaseous counter with multi-anode array can be expressed in a similar way. Formerly hyperbolic sine functions have been used in the analysis of such a counter. The prominence of the present solution over the hyperbolic sine function is examined in the case where the anode-to-cathode distance is comparable or less than the intervals of the anodes. The potential distribution in the rectangular counter and in the multi-anode counter are compared with that of a cylindrical counter. Also is derived the potential distribution in the multi-anode counter with wire-cathodes midway between the anodes, in which a polarization effect on the anode and the wire-cathode is taken into account.

1. Introduction

Recently proportional counters of large sensitive area or of special configuration are widely used in the detection of low energy γ-rays for the purpose of health physics[1–7]) or X-ray astronomy[8]) or in the field of high energy physics to detect the spatial position of penetration by charged particles[9–17]). In these applications proportional counters of rectangular section are often used. Such counters have the advantage over those of cylindrical section in the detection of external source as that simple geometrical relationship to source is feasible in case of side window configuration and that a large sensitive area can be obtained by use of a rectangular counter or by an array of such rectangular proportional counters. However, the proportional counter of rectangular section has some disadvantages. For example, the electric field distribution is not isotropic so that gas multiplication near the anode wire may be anisotropic which may result in poor energy resolution. Moreover the electric field at the corner of the counter is somewhat weaker than the field at the midst of the side of the rectangle. This causes longer drift times of electrons and accordingly causes much chances of recombination in the initial ion track and much chances of negative ion formation through electron attachment to such impurity gases of large electron affinity as oxygen in the way of drift to the anode. Therefore the events occurred at the corner may be recorded smaller, which results in the degradation of the energy resolution[3]). In this sense, energy resolution of the rectangular proportional counter is more sensitive to gas impurity than that of cylindrical counters.

Assuming that the counter is infinitely long in the axial direction of the counter, then the potential is independent of the coordinate parallel to the axial direction, so that the potential problem reduces to a two-dimensional one, which holds for the problems under consideration.

If the plane perpendicular to the axis of the counter is represented by a complex coordinate, then the regular function $W(z) = V(z) + iU(z)$, the real part of which satisfies the boundary condition, is the solution of the potential problem, where the real part, $V(z)$, denotes the potential, and the imaginary part, $U(z)$, is interpreted as integrated electricity measured from some point induced on the surface of the imaginary conductor placed along the equi-potential line[18]). Therefore the charge density on the surface of the conduction electrode can be obtained by differentiation of $U(z)$ along the surface of the electrode. The loci of z on the condition that $V(z) = \text{constant}$ and $U(z) = \text{constant}$ mean the equi-potential lines and lines of force, respectively, so that the inverse transformation of the complex potential function is required to obtain equipotential lines and lines of force.

If the boundary condition, which is too complicated to solve in the original space, is conformally transformed into a simpler one by means of an appropriate regular function and is solved in the mapped space, then the potential function in the original space will be obtained by inverse transformation[24]). This method can be applicable to the problems under consideration by virtue of the Jacobian elliptic function. The potential distribution may serve for the analysis of the problems encountered in the rectangular counters.

Various types of proportional counters with a multi-

anode array, e.g. drift chamber, are used in the field of high energy physics to detect the position of penetration by charged particles[9-17]). Analyses of potential distributions in such counters have been performed by means of the hyperbolic sine function[11,10,18]), which is approximately true in case where the cathode-to-anode distance is much larger than the separation of the anode wires. Several methods have been reported on the deduction of position information by use of gaseous counters acting in the proportional region[9-16]) or slightly above the proportional region[10]). The accuracy of position determination is limited by the wire spacing of the anode array in these counters. Therefore, the need for closer spacing of the anode array may arise. If the closer spacing is adopted, a greater portion of the applied voltage between anode and cathode is allotted to the 'drift region' and, in turn, a share of the applied voltage to 'multiplication region' around the anode wires decreases, which results in the decrease of gas gain. The applied voltage must be raised in order to maintain gas gain, but, on the other hand, we meet with the problem of voltage break down[10]). A solution for these problems is to decrease the anode-to-cathode distance. In practice, the anode-to-cathode distance is comparable to the spacing of a multi-anode in such a geometrical configuration, where the potential expressed in terms of the hyperbolic sine function is no longer valid. The exact potential function is obtained even in such a case in the way analogous to that used in the analysis of the proportional counter of rectangular section. Buchholz[21]) has given a solution to this problem, which is expressed by means of theta-function. Morse and Feshbach[25]) have given another expression to the same problem, which consists of two kinds of elliptic functions with the same periodicity. For calculation of equi-potential lines and lines of force, the inverse transformation of the potential is required, but both expressions are inconvenient for inverse transformation. On the other hand, the present solution is expressed with only one kind of elliptic function, so that inverse transformation is feasible.

Another solution to the contradiction between spatial resolution and gas gain is to arrange a wire cathode between each anode wire[16]), so that the share of the applied voltage to the 'multiplication region' does not decrease, even if the spacing of the anode is reduced. But the adjustment of the voltage of the wire-cathode critically influences the symmetry of the electric field around the anode wire. Sikkem[16]) has given an approximate potential to this configuration using a hyperbolic sine function, in which he does not take account of dielectric polarization on the anode by a charge on the wire cathode and vice versa. Therefore his condition that the potential be constant on the anode is inaccurate, since dielectric polarization on the anode induced by a charge on the wire cathode offsets the potential produced by a charge on wire cathode. The solution in this article takes account of this polarization effect.

2. Potential of a rectangular counter

2.1. Calculation of potential in a rectangular counter

Fig. 1a represents the rectangular cross-section of the counter where the closed line defined by $(K, K+iK', -K+iK', -K)$ denotes the rectangular cathode and point $z = iK'/2$ denotes the anode with electricity $+e$.

Here we apply the conformal transformation (1) to the rectangle shown in fig. 1a,

$$\omega = \mathrm{sn}\, z; \tag{1}$$

then the cathode is mapped to the real axis of fig. 1b, the centre of the anode to $\omega = i/\sqrt{k}$ and the inner portion of the rectangle in z-space to the upper half plane in ω-space. The corresponding coordinates in

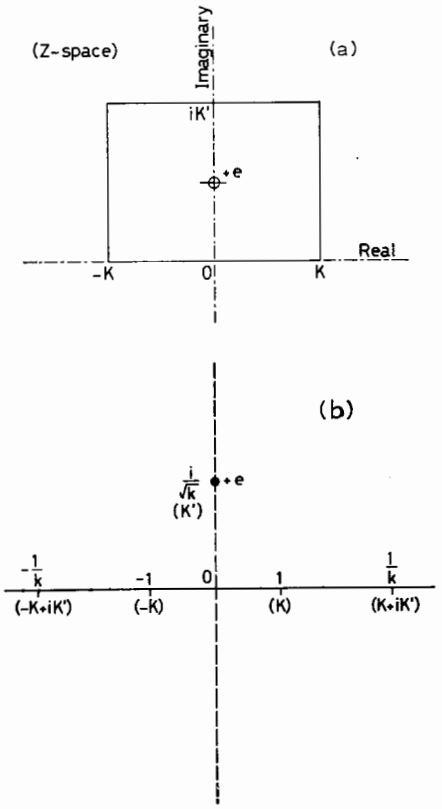

Fig. 1. (a) Cross section of rectangular counter perpendicular to the anode. (b) Mapping of (a) by means of sn-function. In (b) values in parentheses denote corresponding coordinates in (a).

the z-plane are indicated in the parentheses in fig. 1b. Now we apply the method of electrical image to this boundary condition. The potential function $\phi(\omega)$ can be readily calculated as follows,

$$\begin{aligned}\phi(\omega) &= -2e\log(\omega - i/\sqrt{k}) + 2e\log(\omega + i/\sqrt{k}) \\ &= -2e\log[(\omega - i/\sqrt{k})/(\omega + i/\sqrt{k})]. \end{aligned} \tag{2}$$

In representing this potential function in terms of z, we can readily obtain the potential function in z-plane as follows,

$$W(z) = -2e\log\frac{\operatorname{sn} z - i/\sqrt{k}}{\operatorname{sn} z + i/\sqrt{k}}. \tag{3}$$

The function (3) has the same periodicities $4K$, $2iK'$ as that of the sn-function, but has four poles and four zeros.

The potential $V(z)$, the real part of $W(z)$, has some notable properties,

$$\begin{aligned} V(z) = \operatorname{Re}\{W(z)\} &= -2e\log\frac{|(\operatorname{sn} z - i/\sqrt{k})|}{|(\operatorname{sn} z + i/\sqrt{k})|} \\ &= -e\log\frac{(\operatorname{sn} z - i/\sqrt{k})\overline{(\operatorname{sn} z + i/\sqrt{k})}}{(\operatorname{sn} z + i/\sqrt{k})\overline{(\operatorname{sn} z - i/\sqrt{k})}}, \end{aligned} \tag{4}$$

then

$$\begin{aligned} V(-\bar{z}) &= -e\log\frac{[\operatorname{sn}(-\bar{z}) - i/\sqrt{k}]\overline{[\operatorname{sn}(-\bar{z}) + i/\sqrt{k}]}}{[\operatorname{sn}(-\bar{z}) + i/\sqrt{k}]\overline{[\operatorname{sn}(-\bar{z}) - i/\sqrt{k}]}} \\ &= -e\log\frac{(-\operatorname{sn}\bar{z} - i/\sqrt{k})(-\operatorname{sn}\bar{z} + i/\sqrt{k})}{(-\operatorname{sn}\bar{z} + i/\sqrt{k})(-\operatorname{sn}\bar{z} - i/\sqrt{k})} \\ &= V(z), \end{aligned} \tag{5}$$

and

$$\begin{aligned} &V(\bar{z} + iK') \\ &= -e\log\frac{[\operatorname{sn}(\bar{z} + iK') - i/\sqrt{k}]\overline{[\operatorname{sn}(\bar{z} + iK') + i/\sqrt{k}]}}{[\operatorname{sn}(\bar{z} + iK') + i/\sqrt{k}]\overline{[\operatorname{sn}(\bar{z} + iK') - i/\sqrt{k}]}} \\ &= V(z). \end{aligned} \tag{6}$$

Eqs. (5) and (6) indicate that the potential $V(z)$ is symmetric with respect to both the imaginary axis and the Im $\{z\} = K'/2$ axis. Accordingly, only a quarter part of fig. 1a, for example the domain surrounded by the points $(0, K, K + iK'/2, iK'/2)$, is adequate to the analysis of the potential distribution of the whole rectangle. While $U(z)$, the imaginary part of $W(z)$, changes sign through these inversions with constant charge shift, so that the charge density, the derivative along an equi-potential line, is symmetric with respect to the imaginary axis and the Im $\{z\} = K'/2$ axis.

2.2. Calculation of capacitance between anode and cathode

The potential function eq. (3) includes electricities on anode and cathode instead of voltage difference between anode and cathode. Usually the latter is given, so that the capacitance C between anode and cathode is required to the conversion of the voltage difference to electricities. Let r be the radius of the anode wire, then any point Z_a on the surface of the anode can be represented in polar coordinates as:

$$Z_a = re^{i\phi} + iK'/2. \tag{7}$$

Let the voltage difference between the anode and the cathode be V_a, then the potential at the surface of the anode is

$$V_a = \operatorname{Re}\{W(Z_a)\} = -2e\operatorname{Re}\left\{\log\frac{\operatorname{sn} Z_a - i/\sqrt{k}}{\operatorname{sn} Z_a + i/\sqrt{k}}\right\}, \tag{8}$$

while

$$\operatorname{sn}(Za) \pm i/\sqrt{k} \xrightarrow[r \ll 1]{} \frac{1}{\sqrt{k}}[re^{i\phi}(1+k) + i \pm i], \tag{9}$$

so that

$$\begin{aligned} V_a &\xrightarrow[r \ll 1]{} -2e\operatorname{Re}\left\{\log\frac{re^{i\phi}(1+k)}{2i}\right\} \\ &= -2e\log\left|\frac{re^{i\phi}(1+k)}{2i}\right| = -2e\log\tfrac{1}{2}r(1+k). \end{aligned} \tag{10}$$

Hence

$$C = \frac{e}{V_a} = -\frac{1}{2\log\frac{1}{2}r(1+k)}. \tag{11}$$

Hence the potential function can be expressed in terms of the voltage difference between anode and cathode,

$$W(z) = \frac{V_a}{\log\frac{1}{2}r(1+k)}\log\frac{\operatorname{sn} z - i/\sqrt{k}}{\operatorname{sn} z + i/\sqrt{k}}. \tag{12}$$

2.3. Equi-potential lines and lines of force

The loci on the condition the real part of $W(z) =$ $=$ constant and the imaginary part of $W(z) =$ constant represent equi-potential lines and lines of force, respectively[18]), so that next we must calculate the inverse function of eq. (3) in terms of z. By solving eq. (3) with

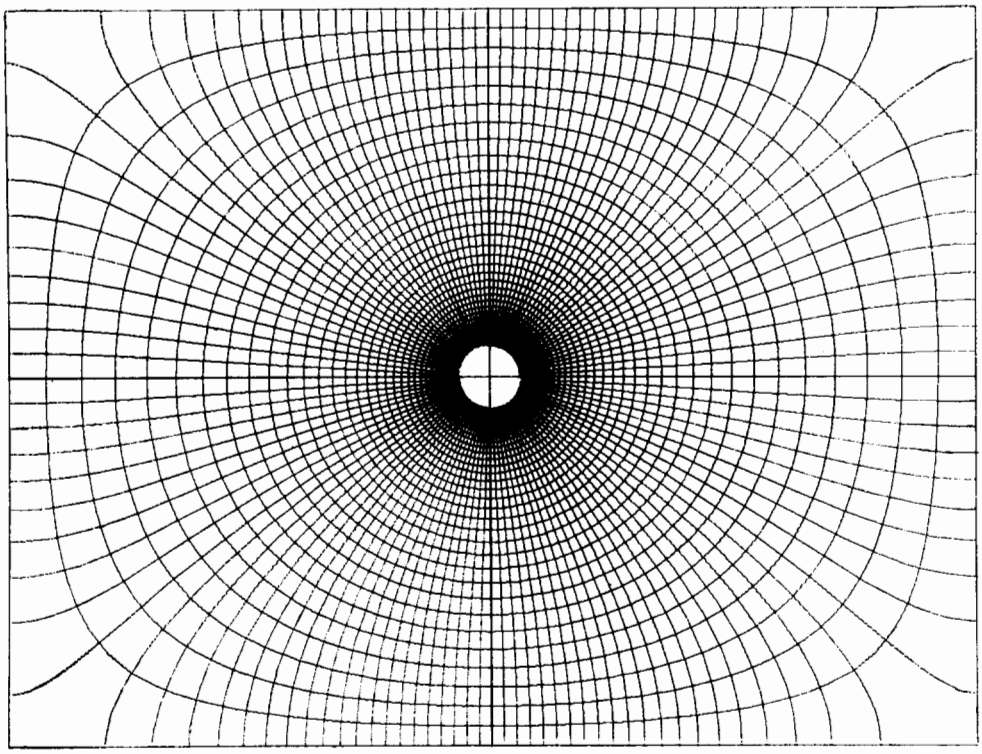

(a)

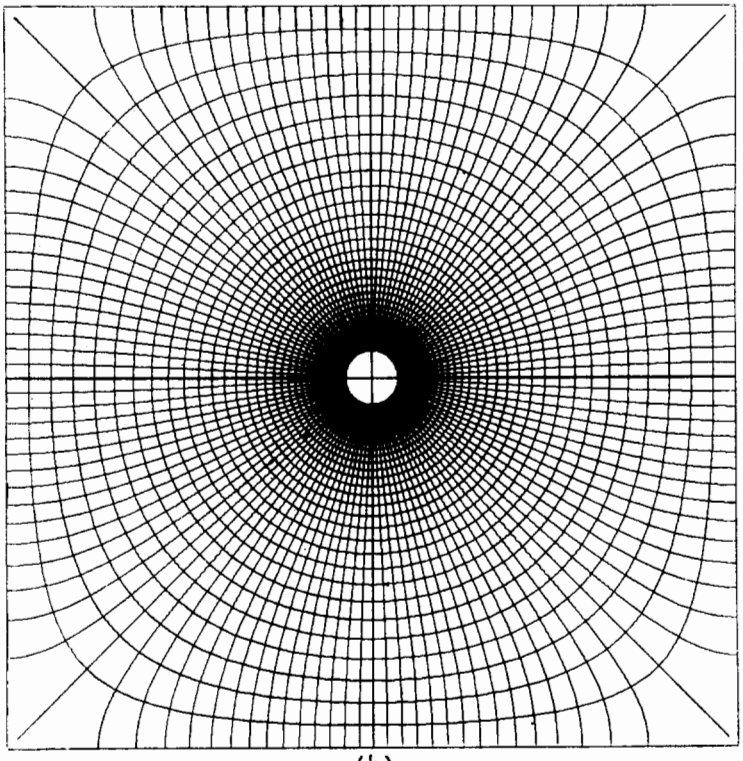

(b)

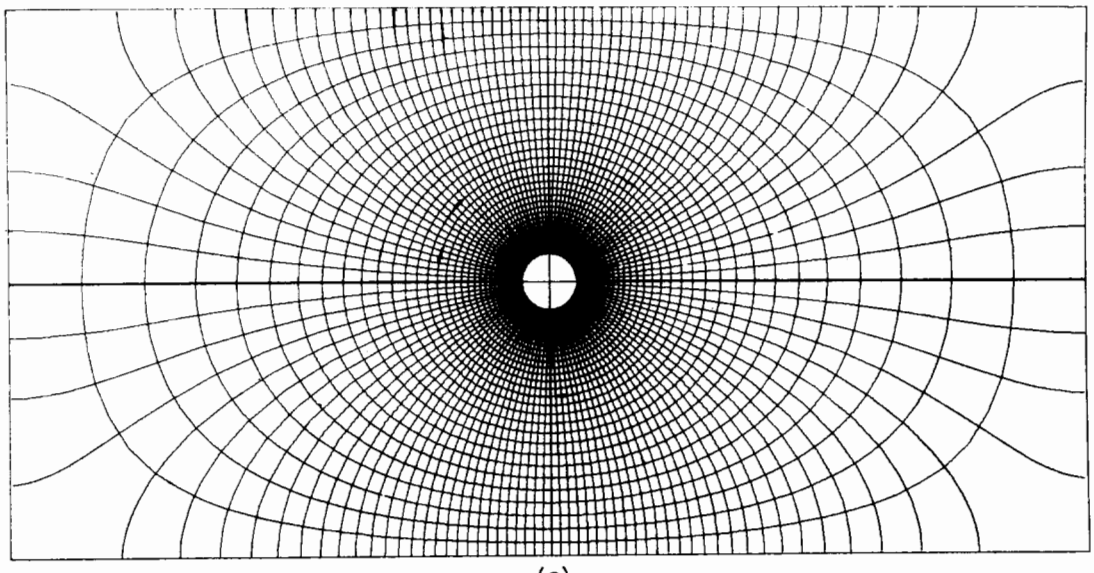

(c)

Fig. 2. Equi-potential lines and lines of force for (a) $K'/K = 1.5$, $r/K = 3.125 \times 10^{-4}$; (b) $K'/K = 2$, $r/K = 3.125 \times 10^{-4}$; (c) $K'/K = 1$, $r/K = 3.125 \times 10^{-4}$, where r, K and K' denote radius of the anode, width and length of the rectangle, respectively. Equi-potential lines and lines of force are shown from a cathode potential up to 30% of the anode potential at intervals of 1% of the anode-to-cathode voltage.

respect to the term sn z, we obtain the following expression,

$$\operatorname{sn} z = -\frac{\mathrm{i}}{\sqrt{k}} \frac{\exp(-W/2e)+1}{\exp(-W/2e)-1}; \tag{13}$$

then z can be expressed in eq. (14) by definition of the Jacobian elliptic function,

$$z = \int_0^u [(1-t^2)(1-k^2t^2)]^{-\frac{1}{2}} \mathrm{d}t, \tag{14}$$

where

$$u = -\frac{\mathrm{i}}{\sqrt{k}} \frac{\exp(-W/2e)+1}{\exp(-W/2e)-1}. \tag{15}$$

Formula (14) can be transformed to

$$\begin{aligned} z &= \int_0^1 [(1-t^2)(1-k^2t^2)]^{-\frac{1}{2}} \mathrm{d}t + \\ &\quad + \int_1^u [(1-t^2)(1-k^2t^2)]^{-\frac{1}{2}} \mathrm{d}t \\ &= K - \int_u^1 [(1-t^2)(1-k^2t^2)]^{-\frac{1}{2}} \mathrm{d}t. \end{aligned} \tag{16}$$

As to the second term, $1/(1-k^2t^2)^{\frac{1}{2}}$ can be expanded into a power series of t, which is uniformly convergent in the region $|t| \leqslant 1/\sqrt{k}$. The integration of the second term in eq. (16) can be performed term by term in this region, which leads to

$$\begin{aligned} Z &= K - (1/\mathrm{i})\, L_0 \log[u + \mathrm{i}(1-u^2)^{\frac{1}{2}}] + \\ &\quad + (1-u^2)^{\frac{1}{2}} \left(L_1 u + \frac{2}{3} L_3 u^3 + \frac{2\cdot 4}{3\cdot 5} L_5 u^5 + \ldots \right), \end{aligned} \tag{17}$$

where

$$\begin{aligned} L_0 &= 1 + (\tfrac{1}{2})^2 k^2 + \left(\frac{1\cdot 3}{2\cdot 4}\right)^2 k^4 + \left(\frac{1\cdot 3\cdot 5}{2\cdot 4\cdot 6}\right)^2 k^6 + \ldots, \\ L_1 &= \quad (\tfrac{1}{2})^2 k^2 + \left(\frac{1\cdot 3}{2\cdot 4}\right)^2 k^4 + \left(\frac{1\cdot 3\cdot 5}{2\cdot 4\cdot 6}\right)^2 k^6 \quad \ldots, \\ L_3 &= \qquad\qquad \left(\frac{1\cdot 3}{2\cdot 4}\right)^2 k^4 + \left(\frac{1\cdot 3\cdot 5}{2\cdot 4\cdot 6}\right)^2 k^6 + \ldots, \\ L_5 &= \qquad\qquad\qquad\quad \left(\frac{1\cdot 3\cdot 5}{2\cdot 4\cdot 6}\right)^2 k^6 + \ldots. \end{aligned} \tag{18}$$

The condition of uniform convergence is

$$\left| -\frac{\mathrm{i}}{\sqrt{k}} \frac{\exp(-W/2e)+1}{\exp(-W/2e)-1} \right| \leqslant \frac{1}{\sqrt{k}}, \tag{19}$$

which leads to

$$\cos(U/2e) \leqslant 0, \tag{19'}$$

i.e.

$$\tfrac{1}{2}\pi \leqslant \tfrac{1}{2}U/e \leqslant \tfrac{3}{2}\pi, \qquad (19'')$$

where $U = \mathrm{Im}\ \{W\}$. Inequality (19″) corresponds to the region $(K, K+\mathrm{i}K'/2, -K+\mathrm{i}K'/2, -K)$ in fig. 1a. The consideration of symmetry of the potential in connection with eqs. (5) and (6) reveals that the potential is symmetric with respect to the imaginary axis and the $z = \mathrm{i}K'/2$ axis. This allows the analysis of only a quarter part of the rectangle to be sufficient, so that we first calculate equi-potential lines and lines of force in the half region of eq. (19″), and then the residual region of the rectangle can be obtained through inversion with respect to these axes. In the actual calculation of the potential in a rectangular counter, length and width of the rectangle and the diameter of the anode are given. $2K$ and K' correspond to the length and width of the rectangle (see fig. 1a), but K and K' can not be given independently, since both K and K' are determined by the same modulus k, so that the only freedom left is to choose the ration K'/K or modulus k. In short, the ratio K'/K or modulus k characterizes the properties of the elliptic integral and the elliptic function. In the case that modulus k is given, K and K' can be calculated by eq. (17).

On the other hand, in case the ratio K'/K is predetermined, k can be calculated with the aid of zero point values of theta functions,

$$k = 4q^{\frac{1}{2}}\left[\prod_{n=1}^{\infty}\left(\frac{1+q^{2n}}{1+q^{2n-1}}\right)\right]^4, \quad \text{where } q = \mathrm{e}^{-\pi K'/K}. \qquad (20)$$

Equi-potential lines and lines of force for $K'/K = 1.5$ and $r/K = 3.125 \times 10^{-4}$ are indicated in fig. 2a. This layout is actually adapted to the proportional counter type lung monitor for the assessment of plutonium lung burden[3]). The physical dimensions are 6 cm × 8 cm rectangle and an anode diameter of 25 μm. The energy resolution of this counter with 90% Ar + 10% methane is 10.2% fwhm for 13.8 keV L X-ray of ^{237}Pu (the daughter nuclide of ^{241}Am), which is in good agreement with the semi-theoretical value[27]) of 10.2% fwhm for monochromatic X-rays. This shows that the energy resolution of a rectangular counter is as good as that of a cylindrical counter, which is also apparent from the potential distribution in fig. 2a.

Also are shown in fig. 2b equi-potential lines and lines of force for $K'/K = 2$, $r/K = 3.125 \times 10^{-4}$ and in fig. 2c, $K'/K = 1$, $r/K = 3.125 \times 10^{-4}$, the former being considered to most resemble the cylindrical counter, the latter being a more eccentric case.

2.4. Comparison of the potential distribution in a rectangular counter with that of a cylindrical counter

It is evident from fig. 2 that equi-potential lines are almost circular near the anode wire. In order to examine the asymptotic functional properties of eq. (3), potential distributions are shown in fig. 3a along representative lines in the rectangle shown in fig. 3b. The potential distribution along lines other than these lines are located between lines (1) and (2), or lines (2) and (3).

The fact that the potential distribution falls on the straight lines up to point R_s in the semi-logarithmic representation indicates that the potential distribution of a rectangular counter resembles that of a cylindrical one. If this straight line is extrapolated to zero potential, R_c the intersection with the r-axis can be regarded as the "cathode radius of equivalent cylindrical counter" given by eq. (21),

$$R_c = 2/(1+k). \qquad (21)$$

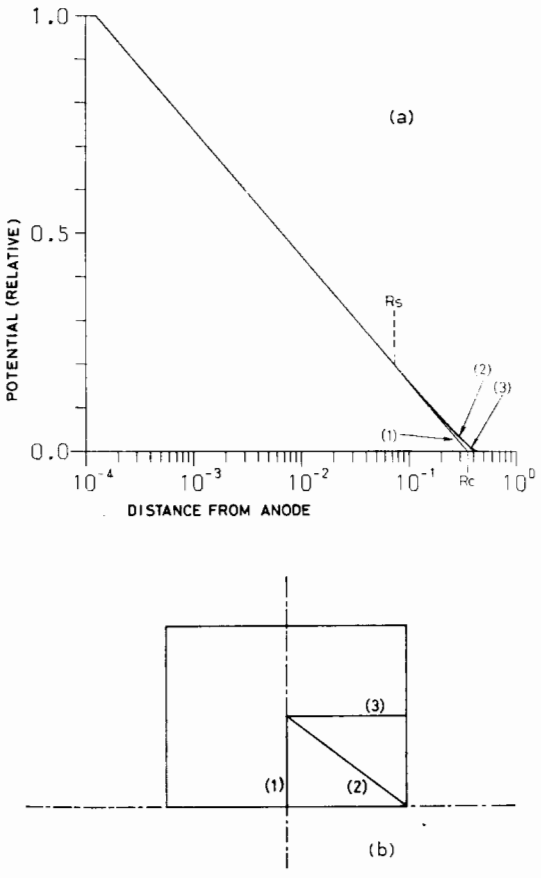

Fig. 3. (a) Potential distributions along the lines in (b).

The asymptotic potential distribution is given by eq. (22).

$$V(z) = \frac{V_a \log(|z|/R_c)}{\log(r/R_c)} = \frac{V_a \log(1+k)\,|z|/2}{\log(1+k)\,r/2}. \quad (22)$$

Eqs. (21) and (22) serve for the estimation of the gas multiplication factor of a proportional counter by means of a theoretical formula [26]), because only the electrical field in the vicinity of the anode is concerned.

3. Potential function of the counter with multi-anode array

3.1. Calculation of potential

Fig. 4a represents the cross-section of the counter with multi-anode array, where the imaginary axis and the Re $\{z\} = 2K$ axis denote cathodes, and points $z = K + inK' + K'/2$ (n: integer) denote anode array electrified with $+e$. Through application of the conformal transformation of eq. (23) to the system shown in fig. 4a,

$$\omega = \mathrm{sn}\, z, \quad (23)$$

then the cathodes and anodes are mapped to the imaginary axis and $\omega = 1/\sqrt{k}$, respectively, as shown in fig. 4b, and the region between two cathodes is mapped to the right half plane in ω-space. In the fig. 4b, corresponding coordinates of representative points in the z-plane are indicated in parentheses. The potential function of the system shown in fig. 4b can be readily obtained by means of the method of electrical image in an analogous way to the case of a rectangular counter,

$$\phi(\omega) = -2e\log(\omega - 1/\sqrt{k}) + 2e\log(\omega + 1/\sqrt{k})$$

$$= -2e\log\frac{\omega - 1/\sqrt{k}}{\omega + 1/\sqrt{k}}. \quad (24)$$

In representing this potential function in terms of z, we can readily obtain the potential function in z-space as eq. (25),

$$W(z) = -2e\log\frac{\mathrm{sn}\, z - 1/\sqrt{k}}{\mathrm{sn}\, z + 1/\sqrt{k}}. \quad (25)$$

It should be noted that "i" in eq. (3) is replaced by "1" in eq. (25). This function has the same periodicities ($4K$, $2iK'$) as the sn-function and is a fourth order elliptic function like function (3) is. The following equations hold for the potential $V(z)$, the real part of function (25),

$$V(-\bar{z} + 2K) = V(z), \quad (26)$$

$$V(\bar{z} + iK') = V(z). \quad (27)$$

These properties of $V(z)$ indicate that the potential $V(z)$ is symmetric with respect to the axis Re $\{z\} = K$ and the axis Im $\{z\} = K'/2$, so that the analysis of only a quarter part of fig. 4a e.g. the domain surrounded by points $(0, K, K + iK'/2, iK'/2)$ is adequate, and potential $V(z)$ in the residual region of unit area can be obtained by inversion of $V(z)$ with respect to the axis Re $\{z\} = K$ and/or the axis Im $\{z\} = K'/2$. While $U(z)$, the imaginary part of $W(z)$, changes sign through these inversions with constant charge shift, so that the charge

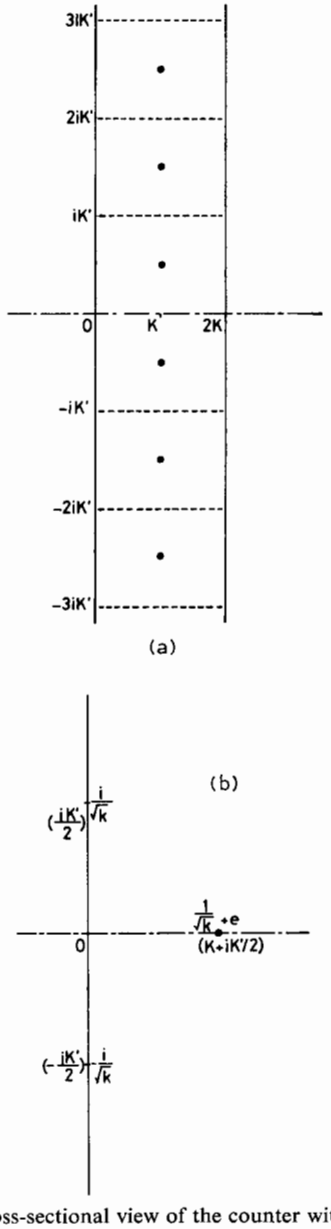

Fig. 4. (a) Cross-sectional view of the counter with multi-anode array. (b) Mapping of (a) by means of sn-function. Values in parentheses indicate corresponding coordinates in (a).

density along an equi-potential line is symmetric with respect to the axis Re $\{z\} = K$ and Im $\{z\} = K'/2$.

3.2. Calculation of capacitance

Capacitance between cathodes and the anode array can be calculated in the way analogous to that adopted in sec. 2.2. A point on the surface of the anode can be represented as:

$$Z_a = r e^{i\phi} + K + iK'/2 + 2inK', \ (n; \text{integer}), \quad (28)$$

and the corresponding potential is

$$V_a = \mathrm{Re}\{W(Z_a)\} = -2e\,\mathrm{Re}\left\{\log\frac{\mathrm{sn}\,Z_a - 1/\sqrt{k}}{\mathrm{sn}\,Z_a + 1/\sqrt{k}}\right\} \quad (29)$$

$$= -2e\,\mathrm{Re}\left\{\log\frac{\mathrm{sn}(re^{i\phi}+K+iK'/2) - 1/\sqrt{k}}{\mathrm{sn}(re^{i\phi}+K+iK'/2) + 1/\sqrt{k}}\right\}$$

$$\xrightarrow[r \ll 1]{} -2e\log|\tfrac{1}{2}re^{i\phi}(1-k)| = -2e\log\tfrac{1}{2}r(1-k),$$

so that

$$C = \frac{e}{V_a} = -\frac{1}{2\log\frac{1}{2}r(1-k)}. \quad (30)$$

Hence the potential function can be expressed in terms of the voltage difference between anode and cathode,

$$W(z) = \frac{V_a}{\log\frac{1}{2}r(1-k)}\log\frac{\mathrm{sn}\,z - 1/\sqrt{k}}{\mathrm{sn}\,z + 1/\sqrt{k}}. \quad (31)$$

3.3. Equi-potential lines and lines of force

By solving eq. (31) with respect to z, one can obtain the following expression for z,

$$z = \int_0^u [(1-t^2)(1-k^2t^2)]^{-\frac{1}{2}}\,dt, \quad (32)$$

where

$$u = -\frac{1}{\sqrt{k}}\frac{\exp(-W/2e)+1}{\exp(-W/2e)-1}. \quad (33)$$

Eq. (32) yields equi-potential lines on the condition Re $\{W\}$ = constant and lines of force on the condition Im $\{W\}$ = constant. Numerical calculation of eq. (32) can be performed in the same way as described in sec. 2.3.

In fig. 5a is shown an example of a potential distribution for $K'/K = 1.5$ and $r/K = 3.125 \times 10^{-4}$. These physical dimensions are the same as those adopted in fig. 2a for the purpose of comparison of the multi-anode counter to the rectangular one. There is a saddle point

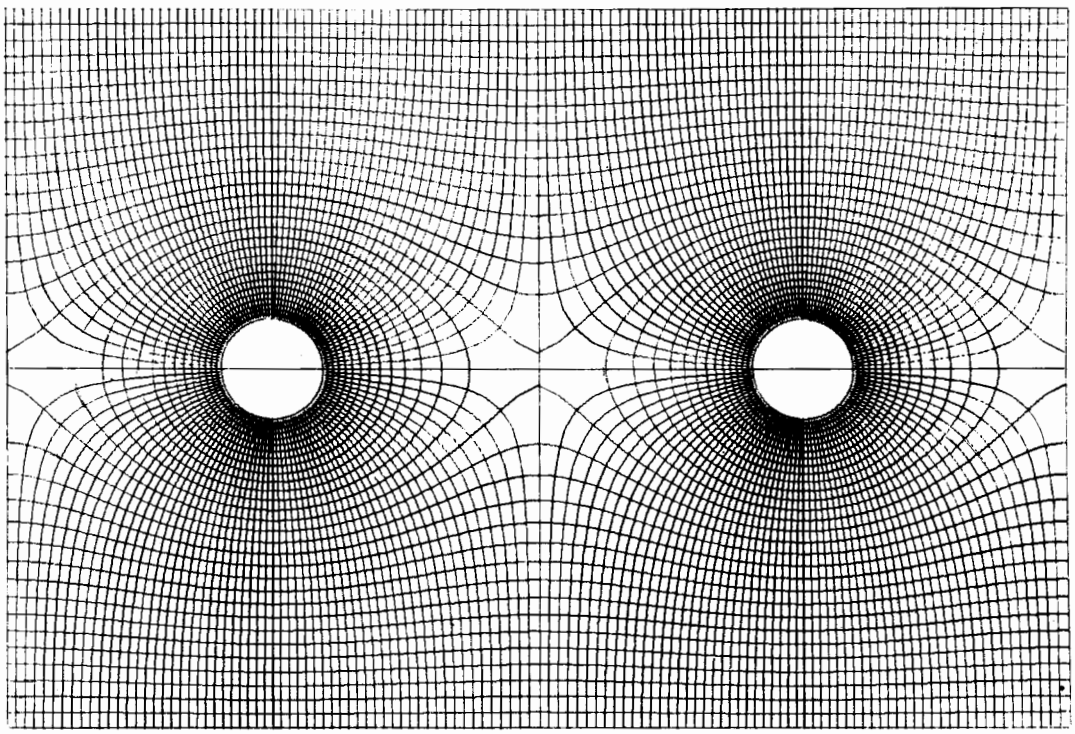

(a)

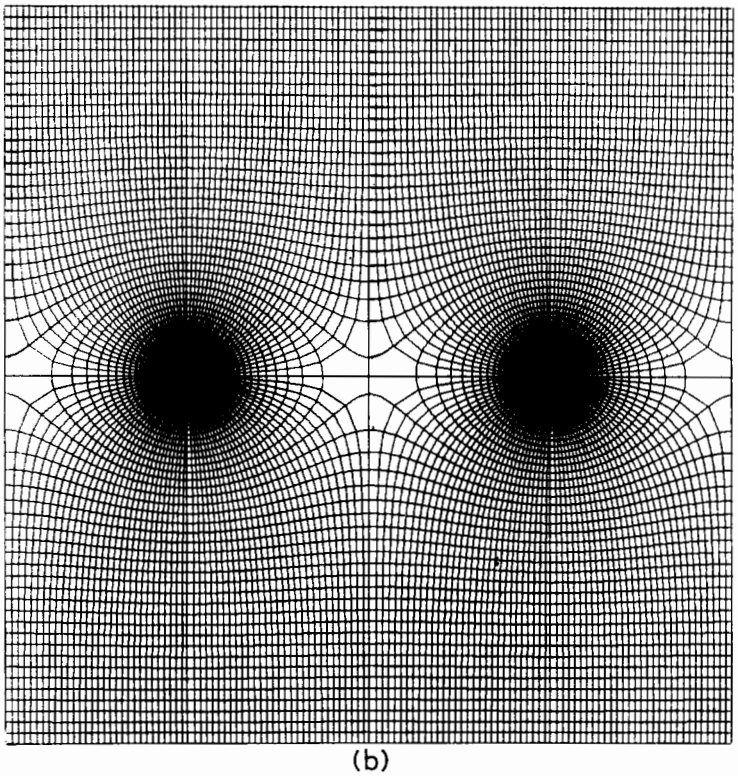

(b)

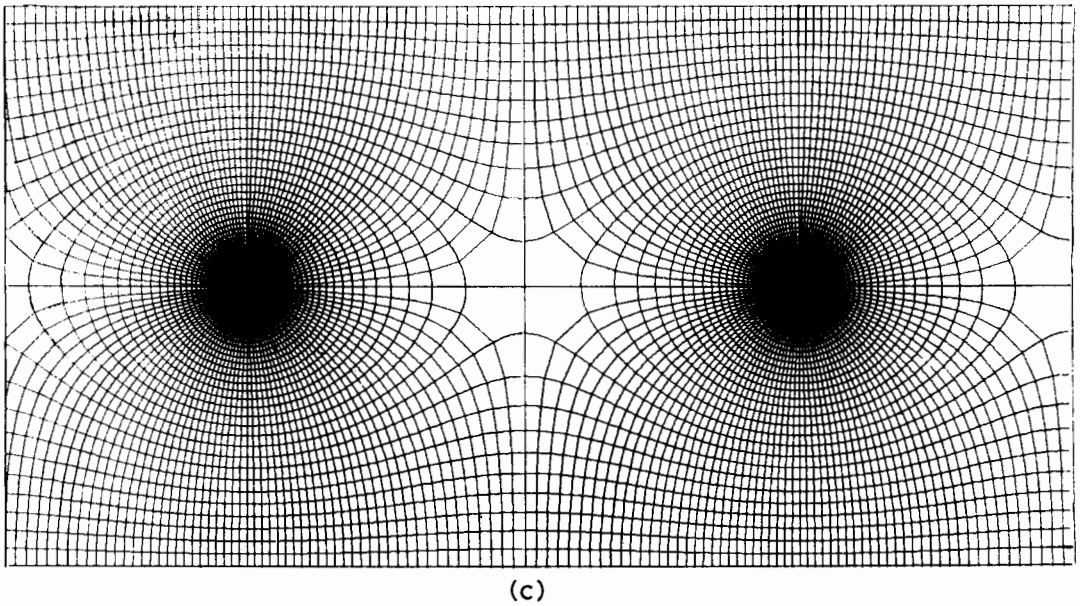

(c)

Fig. 5. Equi-potential lines and lines of force in the counter with multi-anode array for (a) $K'/K = 1.5$, $r/K = 3.125 \times 10^{-4}$; (b) $K'/K = 1$, $r/K = 3.125 \times 10^{-4}$; (c) $K'/K = 2$, $r/K = 3.125 \times 10^{-4}$, where r, K' and K denote radius of anode, length of one section and distance of two cathodes. Equi-potential lines are shown in (a) from a cathode potential up to 30% of the anode potential at intervals of 1% of the anode-to-cathode voltage, while in (b) and (c) from a cathode potential up to 60% of the anode potential at intervals of 1% of the anode-to-cathode voltage.

midway between the anodes, where the electric field is much weaker than in any other portion in the counter.

The potential field can be divided roughly into two portions, one is a "parallel field region" in which the equi-potential lines are almost parallel to the cathodes and the other is a "circular region" in which the equi-potential lines are almost circular around the anode wire. The applied voltage is shared between these two regions, and the potential of saddle point, V_s, is a rough measure of boundary between these regions,

$$V_s = -2e\log\frac{1-\sqrt{k}}{1+\sqrt{k}}. \tag{34}$$

The remarkable difference between fig. 2a and fig. 5a is the fact that a considerable amount of the voltage applied between anodes and cathodes is shared to the parallel field region, while the voltage drop in the vicinity of the anode in the case of fig. 5a is much less than that in the case of fig. 2a. A major part of the applied voltage is alloted to the vicinity of the anode in the case of fig. 2a. In figs. 5b and 5c, potential distributions are shown with $K'/K = 1$, $r/K = 3.125\times10^{-4}$ and $K'/K = 2$, $r/K = 3.125\times10^{-4}$, respectively.

3.4. Equivalent cathode radius

The potential distribution in the vicinity of the anode wire is isotropic as seen in fig. 5, provided that the radius of the anode is much smaller than the spacing of each anode, so that a cylindrical counter approximation holds for the multi-anode counter in an analogous way as described in sec. 2.4.

The cathode radius of an equivalent cylindrical counter is calculated to be

$$R_c = 2/(1-k). \tag{35}$$

This formula may also serve for the estimation of the gas multiplication factor[26]).

3.5. Comparison of the present solution and approximate solution expressed by hyperbolic sine function

It is well known that the potential problem shown in fig. 4a can be represented as eq. (36) with a hyperbolic sine function, provided that the cathodes are located at infinity[18]),

$$W_{hs}(z) = -2e\log(\sinh\pi z/a) + C. \tag{36}$$

If the distance between cathode and anode array is greater than 3 times the spacing of the anodes, the potential function can be approximated by function (36) through adjustment of the constant C such that the boundary conditions at the cathode and anode surfaces are satisfied.

In practice a considerable share of the applied voltage is alloted to the parallel field region in such a configuration, so that the applied voltage must be raised in order to attain a sufficiently high gas gain. Therefore, the need arises to reduce cathode to anode array distance so as to attain high gas gain, which is essential in the case of a position sensitive detector for the purpose of attaining direct position decision making from counter output. In such a case formula (36) is no more valid, while formula (25) is the exact solution.

The numerical calculation of the sn-function in eq. (25) requires as much time as the familiar transcendental function such as the exponential function, since the sn-function can be expressed with theta functions which rapidly converge. Also polynominal (17) rapidly converges so that the elliptic integral (16) can be calculated easily. For example in the case of the geometry in fig. 5a, only 12 terms are sufficient within error of one part per 10^{10}. Hence the calculation of the elliptic integral can be accomplished as easily as that of the sine-function, once modulus k and periodicity moduli K, K' are calculated from given K'/K and then coefficients (18) are calculated.

4. Potential function of multi-anode counter with wire cathodes midway between anodes

In fig. 6a is shown the cross section of such a counter, in which the wire cathodes are arranged midway between the anodes so as to increase the electric field near the anodes. The potential function of this system can be obtained, at first approximation, by superposition of the potential of the system consisting of anodes and plate-cathodes and that of the system of wire-cathodes and plate-cathodes. Here the potential of the wire cathodes is not necessarily at the potential of the plate cathodes, but, on the contrary, the potential of the wire-cathodes is so adjusted that the electric field around the anode becomes isotropic for the purpose of attaining good energy resolution[16]). This approximation is valid everywhere in the counter except near anodes and wire-cathodes,

$$W_p(z) = -2e_1\log\frac{\mathrm{sn}\,z - 1/\sqrt{k}}{\mathrm{sn}\,z + 1/\sqrt{k}} - 2e_2\log\frac{\mathrm{sn}(z-\mathrm{i}K'/2) - 1/\sqrt{k}}{\mathrm{sn}(z-\mathrm{i}K'/2) + 1/\sqrt{k}}. \tag{37}$$

In the vicinity of the anodes and the wire-cathodes, one must take account of the polarization effects

induced on the wire-cathodes by charges on the anode and vice-versa. Let us calculate these polarization effects. The system shown in fig. 6a is mapped into fig. 6b by means of the same transformation as eq. (1) or eq. (23). In fig. 6b, the wire-cathodes and anodes are exaggerated for illustrative purposes. The anode circle at $z = K+iK'/2$ is mapped to the circle at $\omega = 1/\sqrt{k}$ and two semi-circles of wire cathodes at $z = K$ and $z = K+iK'$ to two whole circles at $\omega = 1$ and $\omega = 1/k$ as shown in fig. 6b. Let r_1 and r_2 be the radii of anodes and wire-cathodes, then the radii of the mapped circles R_1 and R_2, R_2' are:

$$R_1 = |\mathrm{sn}(K+iK'/2+r_1)-\mathrm{sn}(K+iK'/2)| \sim (1-k)\,r_1/\sqrt{k}, \quad (r_1 \ll 1), \tag{38}$$

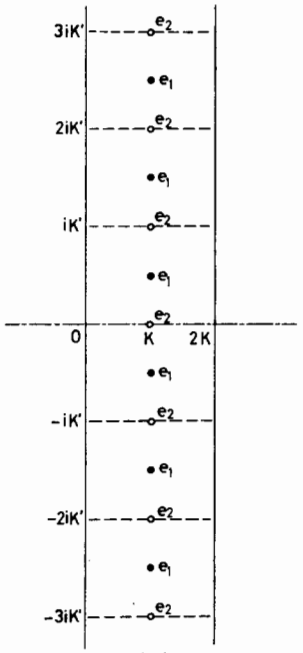

(a)

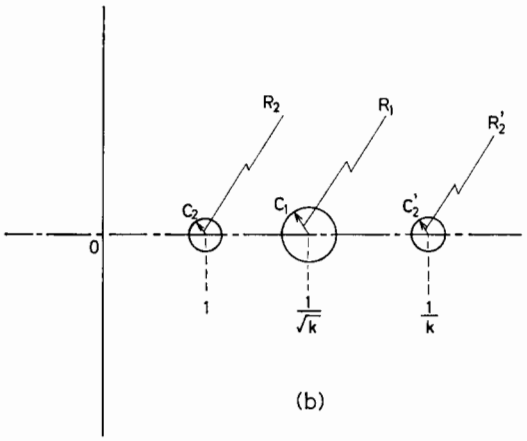

(b)

$$R_2 = |\mathrm{sn}(K+r_2)-\mathrm{sn}(K)| \sim \tfrac{1}{2}(1-k^2)\,r_2^2, \quad (r_2 \ll 1), \tag{38'}$$

$$R_2' = |\mathrm{sn}(K+iK'+r_2)-\mathrm{sn}(K+iK')| \sim \tfrac{1}{2}(1-k^2)\,r_2^2/k, \quad (r_2 \ll 1). \tag{38''}$$

First, let us calculate the polarization on the circle C_2 by a charge e_1 on the anode. The plate-anode is replaced by the electrical image $\overline{A}$ of e_1 at A as shown in fig. 6c. By application of electrical inversion with respect to circle C_2 to this system[18]), e_1 at A and $-e_1$ at $\overline{A}$ are replaced by A′ and $\overline{A}'$. Then,

$$\overline{C_2A'} = \frac{R_2^2}{1/\sqrt{k}-1} = \frac{(1-k^2)^2\,r_2^4}{4(1/\sqrt{k}-1)}, \tag{39}$$

$$\overline{C\overline{A}'} = \frac{R_2^2}{1/\sqrt{k}+1} = \frac{(1-k^2)^2\,r_2^4}{4(1/\sqrt{k}+1)}, \tag{39'}$$

$$\overline{OA'} = 1 + \frac{(1-k^2)^2\,r_2^4}{4(1/\sqrt{k}-1)} \equiv u_1, \tag{40}$$

$$\overline{O\overline{A}'} = 1 - \frac{(1-k^2)^2\,r_2^4}{4(1/\sqrt{k}+1)} \equiv u_2. \tag{40'}$$

Electricities $-e_1$ at A′ and $\overline{A}'$ yield the following potential in ω-space,

$$\phi_{in_1}(\omega) = 2\,e_1 \log[(\omega-u_1)/(\omega-u_2)]. \tag{41}$$

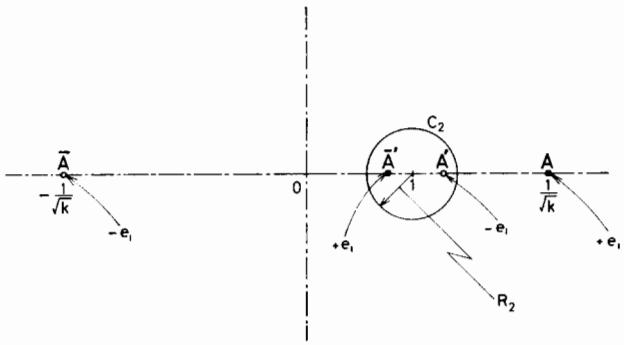

(c)

Fig. 6. (a) Cross-section of multi-anode counter with wire-cathodes midway between anodes. Blank circle and dots denote anodes and wire-cathodes, respectively. (b) Mapping of (a) by means of sn-function. (c) Electrical images of (b) with respect to plate-cathodes at imaginary axis. $\overline{A}$ with charge $-e$ is the electrical image of A with charge $+e$. A′ and $\overline{A}'$ are the electrical inversions of A and $\overline{A}$ with respect to circle C_2, respectively. In this figure cathode C_1 is omitted. Cathode circle C_2 is exaggerated for illustrative purposes.

This yields the following potential in z-space,

$$W_{\mathrm{in}_1}(z) = 2e_1 \log \frac{\mathrm{sn}\, z - u_1}{\mathrm{sn}\, z - u_2}. \tag{42}$$

Similarly, polarization on circle C_2' by a charge e_1 leads to

$$W'_{\mathrm{in}_1}(z) = 2e_1 \log \frac{\mathrm{sn}\, z - u_3}{\mathrm{sn}\, z - u_4}, \tag{43}$$

where

$$u_3 = \frac{1}{k} - \frac{(1-k^2)^2 r_2^4}{4k(1-\sqrt{k})}, \tag{44}$$

$$u_4 = \frac{1}{k} - \frac{(1-k^2)^2 r_2^4}{4k(1+\sqrt{k})}. \tag{44'}$$

In an analogous way polarizations on circle C_1 by charges e_2 at $z = K$ and $z = K + iK'$ yield the following potential functions,

$$W_{\mathrm{in}_2}(z) = 2e_2 \log \frac{\mathrm{sn}(z - iK'/2) - u_1'}{\mathrm{sn}(z - iK'/2) - u_2'}, \tag{45}$$

$$W'_{\mathrm{in}_2}(z) = 2e_2 \log \frac{\mathrm{sn}(z - iK'/2) - u_3'}{\mathrm{sn}(z - iK'/2) - u_4'}, \tag{46}$$

where u_1', u_2', u_3' and u_4' mean that r_2 is replaced by r_1 in eqs. (40), (40'), (44) and (44').

Finally, the total potential can be expressed as;

$$W(z) = W_{\mathrm{p}}(z) + W_{\mathrm{in}_1}(z) + W'_{\mathrm{in}_1}(z) + W_{\mathrm{in}_2}(z) + W'_{\mathrm{in}_2}(z). \tag{47}$$

Terms relating to polarization vanish when the distance from the anode or the wire-cathode is much greater than the radii of anode or wire-cathode. At the surface of the wire-cathode, the superposition term leads to

$$\begin{aligned} W_{\mathrm{p}}(K + r_2 e^{i\phi}) = &- 2e_1 \log[(1-\sqrt{k})/(1+\sqrt{k})] - \\ &- 2e_2 \log \tfrac{1}{2}(1-k) r_2 - 2e_1 i\pi - e_2 i\pi - \\ &- 2e_1(1+\sqrt{k})\sqrt{k}\, r_2^2 e^{2i\phi}, \end{aligned} \tag{48}$$

in which the last term indicates that the potential of simple superposition is not constant at the surface of the conductor. While the potential due to polarization is

$$W_{\mathrm{in}}(K + r_2 e^{i\phi}) = 2e_1(1+\sqrt{k})\sqrt{k}\, r_1^2 e^{-2i\phi}, \tag{49}$$

in which the last term is the potential depending on the angle ϕ of position of the surface of the wire-cathode.

Accordingly total potential is

$$\begin{aligned} W(K + r_2 e^{i\phi}) = &- 2e_1 \log[(1-\sqrt{k})/(1+\sqrt{k})] - \\ &- 2e_2 \log \tfrac{1}{2}(1-k) r_2 e^{i\phi} - 2ie_1 \pi - ie_2 \pi - \\ &- 2e_1(1+\sqrt{k})\sqrt{k}\, r_1^2 (e^{2i\phi} - e^{-2i\phi}). \end{aligned} \tag{50}$$

The real part of eq. (50) is independent of ϕ, so that the potential on the surface of the wire-cathode is constant. In eq. (50) the imaginary part of W represents the integrated charge density on the surface of the wire-cathode, that is,

$$\begin{aligned} -4\pi Q(\phi) &= \mathrm{Im}\{W(K + r_2 e^{i\phi})\} \\ &= -2e_2 \phi - 2e_1 \pi - e_2 \pi - 4e_1(1+\sqrt{k})\sqrt{k}\, r_1^2 \sin 2\phi. \end{aligned} \tag{50'}$$

Therefore the charge density on the surface of the wire-cathode is

$$\begin{aligned} q(\phi) &= \mathrm{d}Q/\mathrm{d}\phi \\ &= e_2/(2\pi) + (2e_1/\pi)(1+\sqrt{k})\sqrt{k}\, r_1^2 \cos 2\phi. \end{aligned} \tag{51}$$

The first term is the charge uniformly distributed around the surface on the wire-cathode and the second term is the induced charge by e_1 on the anode wire. The induced charge distribution is shown schematically in fig. 7, which indicates that the induced charge forms an electric quadrupole on the wire-cathode.

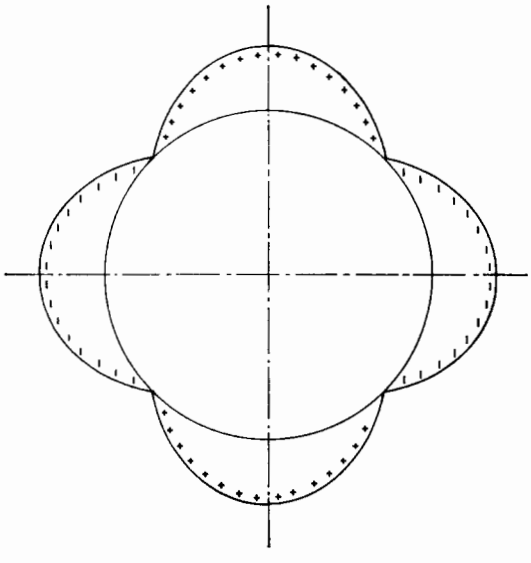

Fig. 7. Induced charge distribution on the wire-cathode. The absolute induced charge is shown by distance from circle at radial direction. (For illustrative purposes only.)

The same argument holds for the surface of the anode, provided that e_1 and r_1 are replaced by e_2 and r_2, respectively.

5. Discussion

It has been demonstrated that conformal transformation by means of Jacobian elliptic function simplifies certain potential problems in two dimensions which have periodicity in two directions. Use of an elliptic function exclusively makes clear the potential distribution in the rectangular counter. In the case of a multi-anode counter the prominence of solution (25) expressed by a sn-function over solution (36) is apparent in the discussion in sec. 3.4. The only error introduced in solution (13) or (25) arises from the finite physical dimension of the anode wire, which is also inherent to the expression (36) with the hyperbolic sine function, although usually the error can be neglected, since the radius of the anode is practically much smaller than the spacing of the anodes, or length or width of the rectangular counter.

There is another approach to the present potential problems. Direct calculation of the potential of electrical images shown in fig. 1a and fig. 4a is feasible. This leads to the results that the potential can be represented by use of theta function. As to the multi-anode counter, the present approach is not applicable to the case in which the anode array is not located midway between two cathode plates and/or the potentials of two cathodes are not equal[21,25]). The latter approach using theta function enables the calculation of the potential in these problems. This method is also applicable to the analysis of the gridded ionization chamber and vacuum triodes. The analysis in this direction may find other fields of application.

References

1) D. Ramsden, Health Phys. **16** (1969) 145.
2) B. Taylor, Health Phys. **17** (1969) 59.
3) T. Tomitani and E. Tanaka, Health Phys. **18** (1970) 195.
4) J. P. Morucci, CEA-R3027 (1966).
5) H. Kiefer and R. Maushart, Atompraxis **14**, no. 8 (1968) 1.
6) P. N. Dean, LAMS-3034.
7) W. H. Tyree, REP-637 (1966).
8) H. Tananbaum and E. M. Kellogg, IEEE Trans. Nucl. Sci. NS-**17**, no. 1 (1970) 97.
9) R. Bouclier, G. Charpak, Z. Dimcovski, G. Fischer and F. Sauli, Nucl. Instr. and Meth. **88** (1970) 149.
10) G. Charpak, D. Rahm and H. Steiner, Nucl. Instr. and Meth. **80** (1970) 13.
11) G. Charpak, R. Bouclier, T. Bressani, J. Favier and C. Zupancic, Nucl. Instr. and Meth. **62** (1968) 262.
12) T. Bressani, G. Charpak, D. Rahm and C. Zupancic, Meeting *Filmless spark and streamer chambers* (Dubna, 15-18 April, 1969).
13) G. Amato, R. Bouclier, G. Charpak, D. Rahm and H. Steiner, Conf. *Spark chambers* (Dubna, 15-18 April 1969).
14) D. Schilly, P. Steffen, J. Steinberger, T. Trippe, F. Vannucci and H. Wahl, private communication.
15) J. H. Dieperink, P. Steffen, J. Steinberger, T. Trippe, F. Vannucci, H. Wahl and D. Zanello, Intern. Conf. *Instrumentation for high energy physics* (Dubna, 8-12 Sept. 1970).
16) C. P. Sikkema, Nucl. Instr. and Meth. **81** (1970) 189.
17) C. J. Borkowski and M. K. Kopp, IEEE Trans. Nucl. Sci. NS-**17**, no. 3 (1970) 340.
18) J. C. Maxwell, *A treatise on electricity and magnetism*, vol. 1 (Dover Publications, New York, 1900).
19) F. B. Vogdes and F. R. Elder, Phys. Rev. **24** (1924) 683.
20) O. Buneman, T. E. Cranshaw and J. A. Harvey, Can. J. Res. A-**27** (1949) 191.
21) H. Buchholz, *Elektrische und magnetische Potentialfelder* (Springer, Berlin, 1957) p. 88.
22) E. Durand, *Electrostatique*, vol. 2 (Massonel, Paris, 1966) p. 308.
23) P. M. Morse and H. Feshbach, *Methods of theoretical physics*, vol. 1 (McGraw-Hill, New York, 1953) p. 425.
24) Ref. 23, vol. 1, p. 443.
25) Ref. 23, vol. 2, p. 1238.
26) M. E. Rose and S. A. Korff, Phys. Rev. **59** (1941) 850.
27) J. Siewert and H. Schmidt, Nucl. Instr. and Meth. **42** (1966) 45.